CHAPTER 3. CO OXIDATION ON A Ru (0001) ELECTRODE

3.1 Introduction

For the last three decades, the elementary step to study electrocatalytic oxidation of C_1 molecules, the electro-oxidation of carbon monoxide (CO), on single Pt and Pt-Ru alloys has been studied in detail both experimentally and theoretically in more than one thousand papers. The role of Pt remains central to electrocatalysis in fuel cell application, with binary Pt-Ru catalysts showing the highest activity toward the oxidation of methanol [70, 84, 85]. Although ruthenium (Ru) is essentially inactive toward the oxidation of methanol [70, 86], it is critical to the activity of the binary catalyst compared with other metals, since it is believed to provide oxygen-containing species at a significantly lower overpotential of *ca.* 300 mV than Pt [87, 88], which can promote CO oxidation. However, CO oxidation on Ru surfaces is not well understood up to now. In the CO oxidation, supported and/or unsupported Ru catalysts were more active compared with single Pt [89], Pd [90], Ir [91] and Rh [92] at high pressures, while at low pressure experiments (*i.e.*, UHV) Ru is the most inactive catalyst [93 – 95]. For a better understanding of the reaction mechanism for CO oxidation on the Ru surface, I tried to find a correlation of the surface structure with the reactivity of CO oxidation on the Ru surface investigated by both structural analysis techniques such as LEED and RHEED/AES and electrochemical methods.

3.2 Experiments

All experiments were performed with a system consisting of a (a) UHV chamber (base pressure $< 1.5 \times 10^{-10}$ mbar) incorporating LEED, RHEED and AES surface analysis, (b) an electrochemical chamber (base pressure $< 1.0 \times 10^{-9}$ mbar), (c) electrochemical cell and (d) a closed sample transfer system (see Figure 3.1). RHEED

was performed with an incident electron beam (40 keV) at a grazing angle of 1 – 2 ^{o} to the surface. The RHEED electron beam also acts as the primary electron source for AES. This combination allows RHEED and AES data to be recorded from the same surface region, thus correlating the structure and chemical composition data (see Refs [96 – 98] for details of experimental procedure and apparatus).

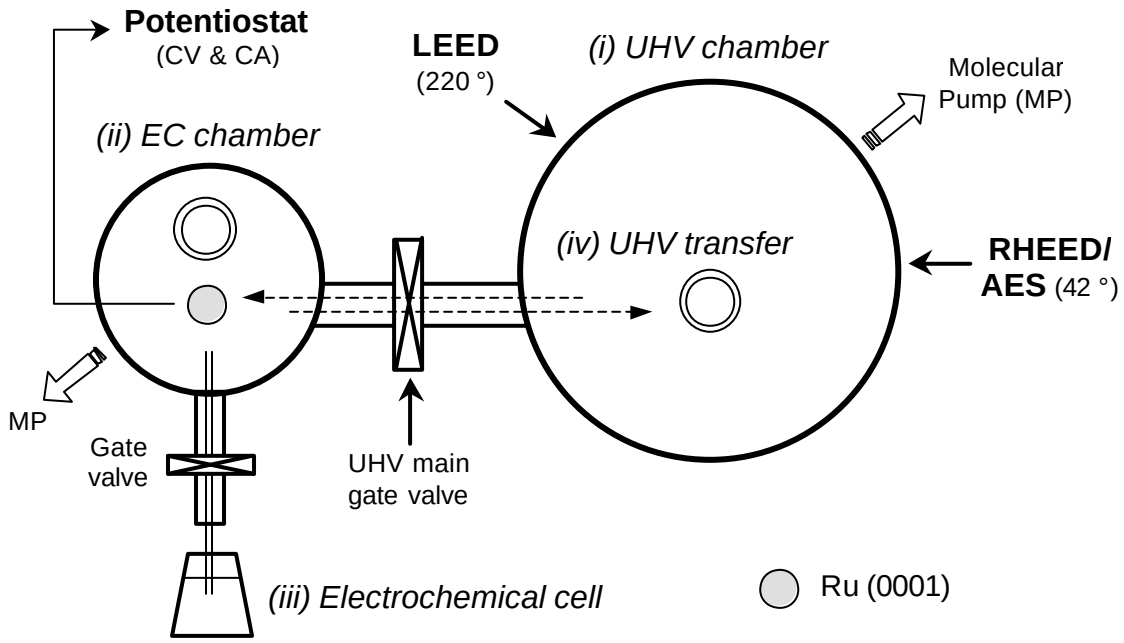

Figure 3.1. Schematic diagram of the UHV electrochemistry transfer system (dashed arrow). (i) UHV chamber (RHEED/AES, LEED), (ii) electrochemical chamber and (iii) electrochemical cell.

3.2.1 Sample pre-treatment

The working electrode, a Ru (0001) single crystal disc of 7 mm diameter (thus exhibiting a geometric area of 0.385 cm^2) and 2 mm thickness, was mounted between tungsten wires, which also served for resistive heating of the sample. To establish a satisfactory electrode pre-treatment procedure that ensures a reproducible state of oxidation, surface morphology and freedom from adsorbed impurities is very important in order to obtain reproducible experimental results. Electrodes are polished on cloth pads impregnated with diamond particles down to 0.7 μm and then with alumina of

fixed grain size down to 0.025 μm. Small particles of alumina may affect the kinetics of a reaction due to the adsorption of reactants on the alumina surface. Particles of polishing abrasives at the Ru surface can be removed by ultrasonic cleaning.

The rough and flat Ru (0001) surfaces were prepared by applying argon ion bombardments at room temperature and 700 °C (at 5×10^{-5} mbar), respectively. The flat surface was subsequently annealed at 1000 °C. The sample surface free from disorder and impurities was examined by LEED/RHEED and AES. The Ru electrode was then transferred to the electrochemical chamber under UHV conditions for the measurement of the cyclic potential sweeping. The electrode surface after the electrochemical treatments and emersion was again characterised by LEED/RHEED and AES.

3.2.2 Electrochemical experiments

The electrochemical setup consists of two cells, and a flow-cell procedure has been used which allows the change of electrolyte solutions under potential control and in an air-free atmosphere. Three-electrode systems and an in-house potentiostat (*ELAB* of Fritz-Haber-Institut) were used for all CVs and chronoamperometry (CA) experiments. A Pt wire of 0.4 mm diameter was used as a counter electrode and placed on top of a glass capillary in the electrolyte vessel [96]. The electrosorption of CO was achieved by immersion of the Ru (0001) electrode in a CO-saturated 0.1 M $HClO_4$ solution at an optimal adsorption potential of − 0.10 V for 2 min. All potentials used are given versus the Ag/AgCl electrode in saturated KCl solution.

3.3 CO oxidation on Ru (0001) surfaces

3.3.1 Cyclic voltammetry of smooth and rough Ru (0001) surfaces

The UHV prepared Ru (0001) surface exhibited a well-ordered flat (1×1) phase, as shown by LEED and RHEED in Figures 3.2(a) and 3.2(b). 2D–reflection rods in RHEED pattern are clearly seen, suggesting a smooth and flat Ru (0001) surface.

Figures 3.3(a) and 3.3(b) show the AES data of Ru and oxygen after sample pre-treatment, respectively. This result shows that all experiments were performed on a clean Ru surface without any impurities. In particular, there are no distinct peaks in Figure 3.3(b), which might indicate the presence of oxygen.

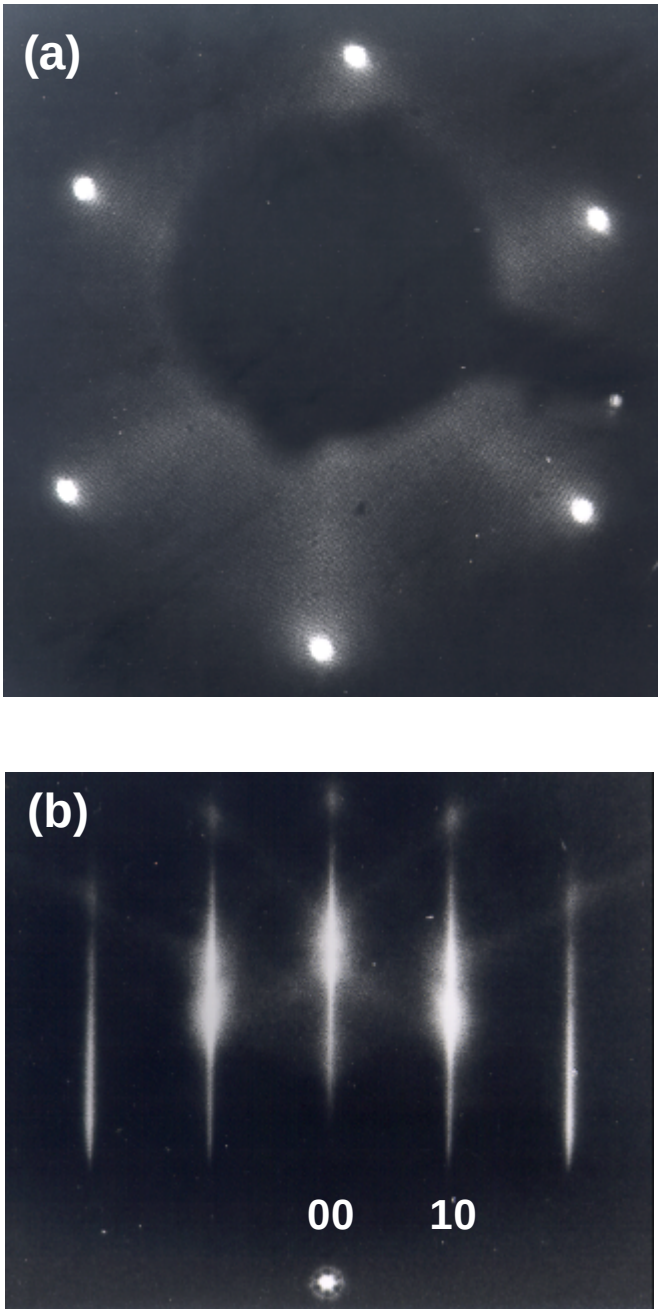

Figure 3.2. (a) LEED (62 eV) and (b) RHEED ([1120] azimuth) patterns for a smooth Ru (0001) electrode prepared by argon ion bombardment at 700 °C and subsequent annealing at 1000 °C.

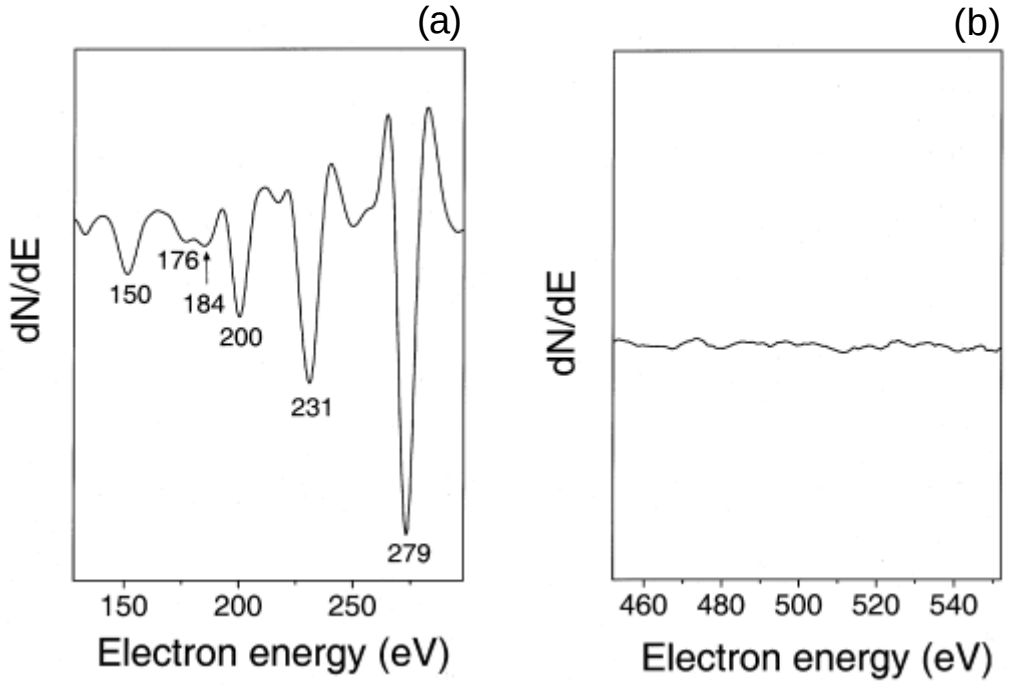

Figure 3.3. Secondary Auger electron spectra of the clean Ru (0001) surface. (a) Ru peaks and (b) oxygen peaks (expected at 512 eV).

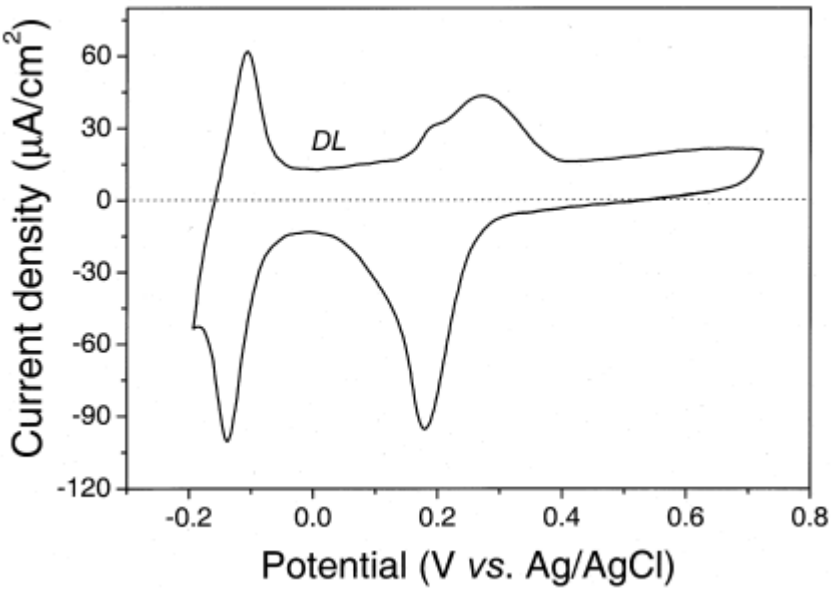

Figure 3.4. Cyclic current-potential curve for a smooth Ru (0001) electrode prepared by argon ion bombardment at 700 °C and subsequent annealing at 1000 °C under UHV conditions in 0.1 M $HClO_4$ with a scan rate of 50 mV/s.

The cleanliness of the Ru electrodes was also characterised by cyclic voltammetry in 0.1 M $HClO_4$. In reproducible CV data (Figure 3.4), the hydrogen adsorption and OH adsorption at – 0.14 V and + 0.25 V are observed, respectively. This CV also shows very low current density at the double layer region, marked with *DL*, ranging between – 0.05 V and + 0.1 V. The above two experimental observations indicate a clean and well-defined flat Ru (0001) surface, which is clearly different from the CV on polycrystalline Ru and the rough Ru electrode surface [99, 100]. Prior to performing the CO stripping voltammetry, the Ru (0001)–(1×1) electrode surfaces were characterised by both surface science techniques (LEED/RHEED and AES) and electrochemical cyclic voltammetry as shown in Figures 3.2, 3.3 and 3.4.

The charge of the cathodic current peak at – 0.14 V is *ca.* 120 μC/cm^2 and it corresponds to 0.5 monolayer (ML) of hydrogen coverage. The remaining Ru surface has apparently been occupied by oxygen species as becomes evident from the (2×2)–O LEED/RHEED patterns of the Ru electrode emersed at + 0.1 V before H adsorption. This indicates an oxygen coverage of 0.5 ML due to Auger O/Ru intensity ratio ($I_O/I_{Ru\,(230)}$) of 0.04 when $I_O/I_{Ru\,(230)}$ of 0.08 corresponds to one monolayer of oxygen showing a (1×1)–O phase. Thus, the structure of Ru at E< 0.2 V and at E > 0.3 V are assigned to (2×2) and (1×1) phases, respectively.

The roughness of the Ru (0001) surface prepared by argon ion bombardment at room temperature, without simultaneous subsequent heating and annealing under UHV conditions, is clearly demonstrated by its RHEED pattern (Figure 3.5). It shows a strong intensity modulation along the reciprocal lattice rods in the RHEED, indicating high surface roughness. This implies that a Ru (0001) surface with numerous defects, facets, steps and kinks is generated by applying Ar^+ sputtering. Figure 3.6 shows no redox couples of H and OH at *ca.* – 0.14 V and + 0.25 V, respectively on the rough Ru (0001) surface. A strongly distorted electrode surface, generated by redox cycles in the oxidation region, results in a broadening of the peak profile for H adsorption/desorption, as already found at the planes of (hkl) of Pt [101] and Au [102]. The broad peak around the double layer region results from the overlap of hydrogen adsorption and hydroxide adsorption peaks that occur at the various facet planes (hkl) of the Ru electrode surface induced by Ar^+ ion sputtering.

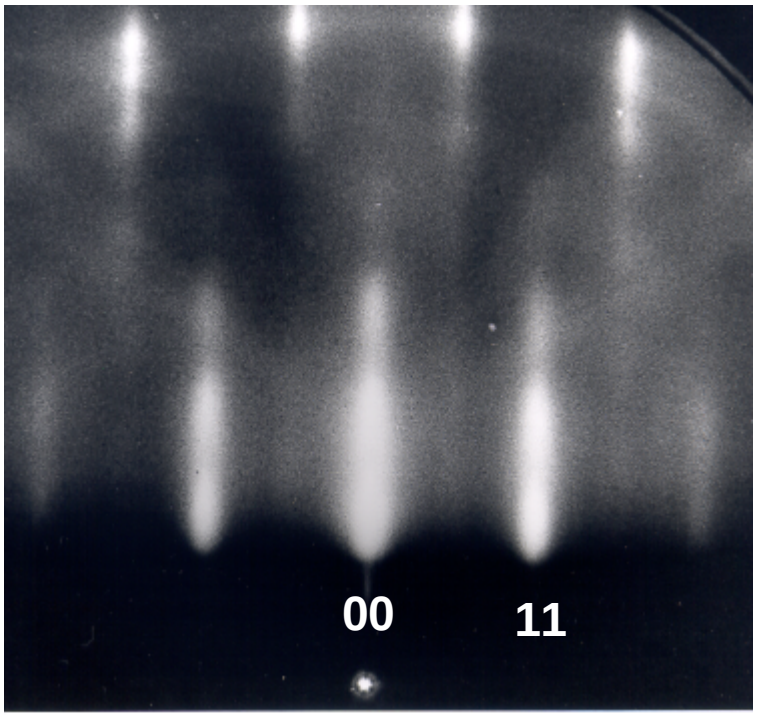

Figure 3.5. RHEED pattern ([0110]) obtained from a rough Ru (0001) electrode surface after argon ion bombardment at room temperature without subsequent annealing under UHV conditions, showing intensity modulation along the reciprocal lattice rods.

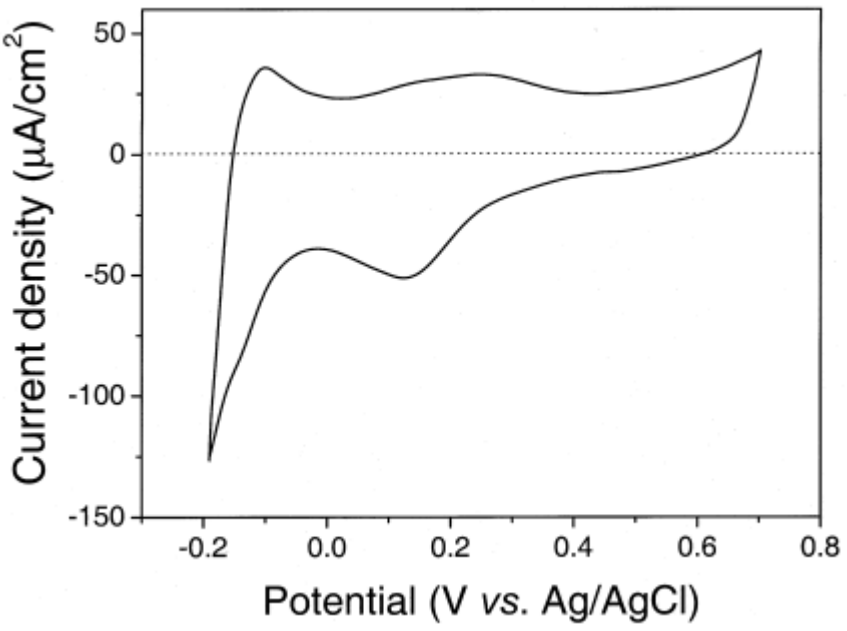

Figure 3.6. Cyclic current-potential curves for a rough Ru (0001) electrode surface prepared by argon ion bombardment at room temperature under UHV conditions in 0.1 M $HClO_4$ with a scan rate of 50 mV/s.

The voltammetric profile in Figure 3.6 resembles the CVs on a polycrystalline Ru electrode [99] and on a polished Ru (0001) electrode prepared in our laboratory (not shown) and data by Lu *et al*. [100]. It is also very similar to the CV profile recorded on a 0.85 ML deposited Ru/Au (111) with many grain boundaries as seen in STM images [103]. However, Figure 3.6 differs remarkably from the CV reported by Lin *et al*. [104], which was obtained from a Ru (0001) electrode polished with 0.015 μm alumina. This showed a very sharp current peak corresponding to the adsorption/desorption of hydrogen. The origin of this discrepancy is not yet clear.

3.3.2 Electro-oxidation of CO_{ad} on a flat Ru (0001) surface

The electrosorption of CO_{ad} on the Ru (0001) electrode was performed by applying the optimum potential of -0.1 V for 2 min in a CO-saturated $HClO_4$ solution. The CV in CO-saturated $HClO_4$ solution (see dotted line in Figure 3.7(a)) for the CO covered Ru (0001) electrode no longer shows H_{ad} and OH_{ad} peaks, due to the complete blocking of adsorption of H and OH by CO_{ad} species; *i.e.*, the presence of a CO adlayer on Ru (0001) results in a strong reduction of the double layer current density in the region between -0.2 V and $+0.3$ V [105]. Subsequently, the CO solution in the electrolyte vessel and the glass capillary was exchanged by a CO free $HClO_4$ electrolyte by means of the flow-cell procedure under air-free atmospheric conditions [106]. The adsorbed CO was then oxidised during cyclic voltammetry with a scan rate of 50 mV/s. The positive potential limits of $+0.9$ V and $+0.7$ V were chosen so as to strip the pre-adsorbed CO from the flat Ru (0001) and the rough Ru (0001) electrode surfaces, respectively, and in order to avoid irreversible disordering of the surface by the place exchange of OH and Ru.

The stripping voltammetry curve of saturated CO_{ad} (0.5 ML) on a flat Ru (0001) in 0.1 M $HClO_4$ is presented in Figure 3.7(a). There is no peak around $+0.25$ V, indicating that the formation of OH_{ad} is blocked by preadsorbed CO. The anodic current increases gradually at $+0.4$ V, and a pronounced peak appears at $+0.8$ V on the first anodic scan, which is ascribed to electro-oxidation of CO_{ad} on Ru (0001), since there is no visible anodic peak at $+0.8$ V in the absence of adsorbed CO on Ru (0001) (as seen in Figure 3.4). On the second cycle, a new anodic peak was obtained at a relatively low overpotential of $+0.55$ V where the oxidation of residual CO_{ad} by O adspecies occurred,

but the anodic peak at + 0.8 V was almost absent. The concomitant adsorption of OH_{ad} is indicated by the reduction peak at + 0.17 V on the first negative-going scan, which is clearly associated with the reduction of the O/OH_{ad} species created during oxidative removal of CO_{ad}. On the 3rd scan, the CO coverage had been reduced sufficiently, so that the OH adsorption manifests itself as a small peak around + 0.25 V; CO oxidation now sets in shortly afterwards, with its peak maximum at + 0.46 V (A similar result for onset potential dependence on CO coverage has also been investigated for CO electro-oxidation on Pd (111) [107]). The results indicate that CO oxidation requires coadsorbed oxygen species. For high CO coverage, oxygen adsorption can only be enforced at large overvoltage (1st scan). At lower coverage, the oxidation sets in much earlier, the additional shift from + 0.55 V to + 0.46 V may be due to variations in binding energy for different O_{ad}/CO_{ad} mixtures. The change of the CO_{ad} bonding state induced by oxidative removal of CO_{ad} is supported by *in-situ* IR measurements [106]. These show coverage dependence of ν_{CO} for a CO adlayer on the Ru electrode similar to the results observed for the change in ν_{CO} on Pd (111) by partial electro-oxidative removal of CO_{ad} [107]. These results suggest that different bonding states of O/CO_{ad} on the Ru (0001) surfaces due to different coverage ratios of O/CO, do not co-exist on the Ru surface under steady state conditions; *i.e.*, the bonding states of O/CO_{ad} adlayers appearing in the second and third cycles are created as a result of oxidative removal of CO_{ad} *via* a relaxation process or a rearrangement of the CO_{ad} adlayer with the coadsorbed oxygenated species.

In order to investigate the dependence of the onset oxidation potential of CO on the coverage of CO on flat Ru (0001), a relatively lower coverage of CO on Ru (0001) was prepared by applying − 0.1 V for 10 sec in a CO-saturated $HClO_4$ solution. The resulting cyclic voltammetric profile of the Ru (0001) electrode is shown in Figure 3.7(b). It is distinctly different from the cyclic voltammetry for a saturated CO coverage of 0.5 ML seen in Figure 3.7(a). The first onset of CO electro-oxidation occurred at a lower overpotential, + 0.55 V, during the first cycle, at the same potential as the second wave in Figure 3.7(a) which occurred after partial removal of CO_{ad} by the first cycle. Thus, the onset of CO oxidation is strongly dependent on coverage.

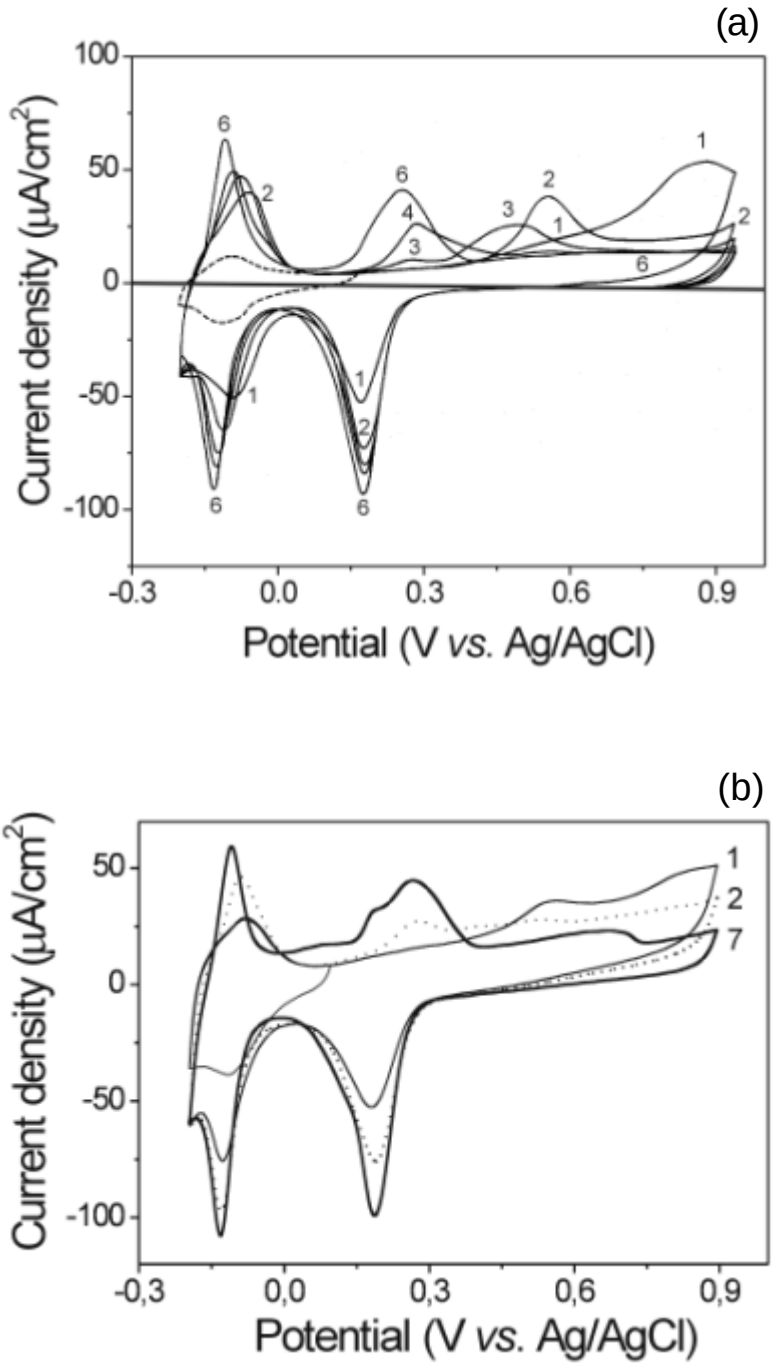

Figure 3.7. Cyclic CO stripping voltammetry [105] on a smooth Ru (0001) electrode with (a) a saturated CO coverage (0.5 ML) and (b) a lower coverage of CO (0.2 ML) in CO free 0.1 M $HClO_4$. Scan rate is 50 mV/s. Sequence of scans is indicated by numbers.

3.3.3 Electro-oxidation of CO on a rough Ru (0001) surface

The CO stripping voltammetry on a rough Ru (0001) electrode is shown in Figure 3.8. The electro-oxidation of CO commences at + 0.15 V and a pronounced broad peak appears around + 0.35 V. Interestingly, it resembles the CV recorded for CO electro-oxidation on a Ru deposited Au (111) electrode surface in 0.1 M H_2SO_4 solution [103]. Thus, we assume that the sputtered Ru (0001) surface has a similar surface morphology as this Ru-modified Au (111). A complete oxidation of the CO monolayer on rough Ru (0001) was achieved by only one oxidative stripping, and it is similar to the result observed at a Ru-modified Au (111) surface [103]. However, this differs from that observed on a flat Ru (0001) surface as shown in Figure 3.7(a), where the adsorbed CO was completely removed only after more than three oxidative stripping cycles.

Note that in a CO-free electrolyte OH formation reached its peaks already at + 0.19 V. The oxidation of preadsorbed CO sets in at about the same voltage. Thus, there is no significant inhibition of adsorption of oxygen species on a rough surface, even when saturated with CO_{ad}.

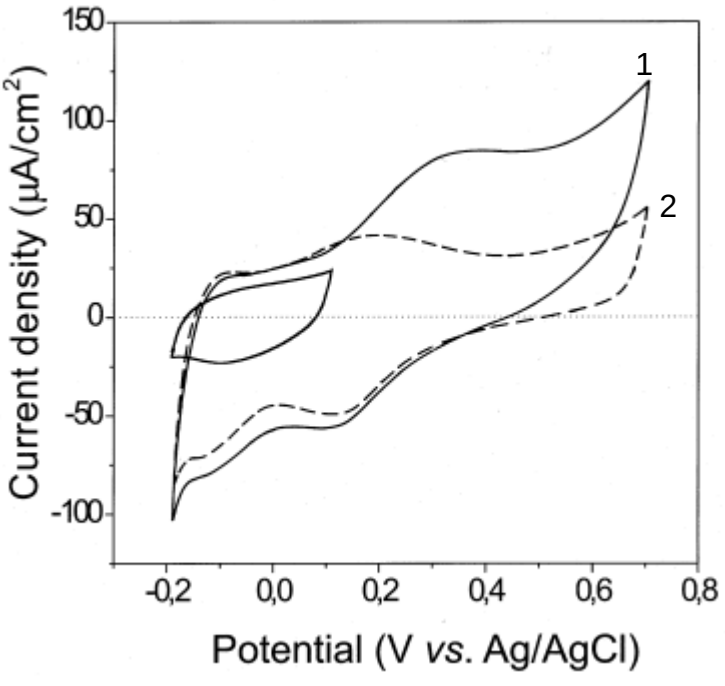

Figure 3.8. Cyclic CO stripping voltammetry (full line) on a rough Ru (0001) electrode in CO free 0.1 M $HClO_4$. Sequence of scans is indicated by numbers.

In order to obtain additional information on the chemical composition on the Ru electrode surface, which could not be obtained from the electrochemical methods, *ex-situ* AES measurements were performed for the Ru electrodes emersed at various electrode potentials. The Auger O/Ru intensity ratio (I_o/I_{Ru}) for the rough Ru(0001) electrode emersed at + 0.3 V is approximately 3 times higher than that obtained from a flat Ru electrode. This suggests that an oxygen adlayer is already formed at + 0.3 V on a rough Ru surface, corresponding in coverage to the O adlayer formed at + 0.7 V on a flat Ru electrode surface. Furthermore, diffuse (1×1) patterns with increased background intensity observed in LEED/RHEED indicated the formation of an amorphous oxide layer on a rough Ru (0001); this was clearly present in the STM image for the Ru deposited Au (111) surface at the same potential range [103]. This oxide layer on a rough Ru surface differs from the (100) RuO_2 oxide formed on a flat Ru (0001) surface at $E > + 1.0$ V where the crystalline oxide was formed with concomitant Ru dissolution as evidenced by RHEED [108]. The higher oxygen coverage on a rough Ru (0001) decreases the overpotential of CO oxidation.

3.3.4 Current-time transients of CO electro-oxidation on a rough Ru (0001) electrode

Not surprisingly the current-time transients of CO oxidation on a flat Ru (0001) surface depend strongly on the applied overpotential [109]. For the comparative study of the oxidation rate of CO_{ad} on a rough Ru (0001) surface with that on a smooth Ru surface, the current responses at four different oxidation potentials were measured on a rough Ru electrode. Figure 3.9(a) shows current-time transients for the oxidation of adsorbed CO on a rough surface at a potential of +0.4 V. For reference, the dotted current-time curve, in 0.1 M $HClO_4$ before the electrosorption of CO on rough Ru (0001) represents the double layer charging and oxidation charging currents. After a sharp increase, the transient (solid line) in Figure 3.9(a) decays for several seconds and then reaches the steady state current value. After subtracting the double layer current, the charge for only CO oxidation is 259 $\mu C/cm^2$ and it corresponds to *ca.* 0.5 ML of CO oxidation on a flat Ru (0001) surface [109]. From comparison of CO oxidation on a

smooth Ru (0001) surface with a saturated CO coverage of 0.5 ML [109] with this higher oxidation rate of CO at + 0.4 V, a roughness factor of two can be estimated.

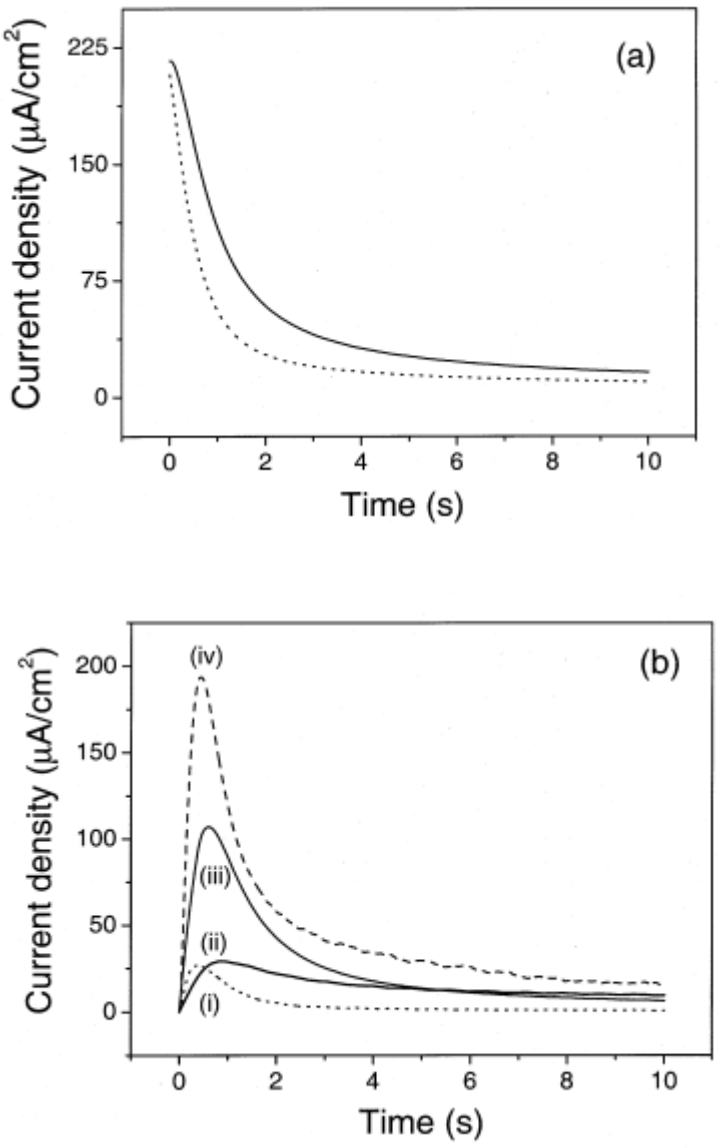

Figure 3.9. (a) Current-time transient for a rough Ru (0001) with a saturated CO coverage in 0.1 M $HClO_4$ solution. The potential step was from –0.1 V to + 0.4 V (*vs*. Ag/AgCl). The double layer and oxidation charging in CO free $HClO_4$ was given by the dashed line. (b) Current-time transients for a CO covered rough Ru (0001) electrode after subtraction of the double layer and oxidation charging for various potentials (+ 0.17 V, + 0.26 V, + 0.4 V and + 0.6 V marked with (i), (ii), (iii) and (iv), respectively).

In Figure 3.9(b), the CO oxidation charge at + 0.17 V for an applied time of 10 s is 43 μC/cm^2, which indicates that 0.084 ML of CO can be oxidised. This charge for CO oxidation significantly increases at higher oxidation overpotential. A high oxidation charge of 446 μC/cm^2 is obtained at + 0.6 V and it is attributed to *ca.* 0.87 ML adsorbed CO on the rough Ru electrode. On the other hand, there were no detectable current-time transients for CO oxidation even at + 0.55 V on flat Ru (0001). These characteristics are consistent with responses that have been observed in cyclic voltammetry measurements (see Figure 3.8) involving CO oxidation. Note that the kinetics of CO oxidation on a Ru (0001) surface depends on facets, defects, and steps generated by Ar^+ sputtering.

Electrocatalytic Oxidation Charge of CO Q_{CO} (μC/cm^2)		
Overpotential (E_{app})	Rough Ru (0001)	Flat Ru (0001)
+ 0.17 V	43	–
+ 0.26 V	150	–
+ 0.40 V	259	–
+ 0.60 V	446	83
+ 0.75 V	Ru oxide	161
+ 0.95 V	Ru oxide or O_2 ↑	226

Table 3.1. The CO oxidation charge calculated from the current-time transients (chronoamperometry) on flat (see Ref. [109]) and rough Ru (0001) electrodes at different oxidation overpotentials.

Table 3.1 summarises the charge of the current transients for CO oxidation on rough and flat Ru (0001) electrodes and the following interesting fact was noted. On a rough Ru (0001) surface, the charge for CO oxidation even at a very low overpotential (+ 0.17 V) is observed, unlike CO oxidation on flat Ru (0001). As already mentioned above, we obtain *ca.* 0.5 ML oxidation current at + 0.4 V on a rough Ru (0001) electrode, and this value can only be achieved at + 0.95 V on a flat Ru surface. At $E_{app} \geq$ + 0.65 V, rough Ru can be oxidised, at about + 0.8 V oxygen evolution started.

3.3.5 Discussion

Electro-oxidation of CO on a flat Ru (0001) surface

In order to rationalise the present experimental results, same remarks on the earlier studies of CO electro-oxidation on a Ru-modified Au (111) electrode are needed. Both electrodeposited Ru and polycrystalline Ru electrode surfaces have always shown a structureless profile for CO stripping voltammetry. Unlike previous studies, the present CV for CO oxidation on flat Ru (0001) exhibits well-characterised anodic/cathodic peaks of H and OH, which allows the study of the change in bonding states of CO/OH adspecies on flat Ru (0001). Although there is a lack of information concerning the bonding energies of O–Ru and CO–Ru in the electrolyte, the ratio of the bonding energy O–Ru/CO–Ru under both UHV and high-pressure conditions may be compatible to those in an electrochemical system. The adsorption/desorption energy of CO on Ru (0001) decreases from 25 kcal/mol to 11 kcal/mol (0.48 eV) from an O–(2 × 1) to an O–(1 × 1) phase under UHV conditions [110]. A similar result [109] has been observed for the electrosorption of CO at + 0.45 V on Ru (0001)–(1 × 1)–O, and this indicates a high mobility of CO on an O–(1 × 1) phase. On the other hand, binding energies of the O/Ru (0001) and O/RuO_2 (110) are 5.8 eV and 3.2 eV, respectively [111, 112], which are substantially larger than the binding energy of CO–Ru.

As shown in section 3.3.1, the current density in the double layer region decreased markedly after CO electrosorption, indicative of the presence of CO_{ad} on the Ru (0001) surface. Up to + 0.5 V, no discernible current peak appeared in the CO stripping voltammetry on a CO + O/OH precovered Ru (0001) surface, as also

confirmed by the current transient measurements [109]. A pronounced peak first appeared at +0.85 V, indicating that the extra energy for the *sluggish* onset of the oxidation process is evidently provided by the overpotential. Apart from the measured anodic current, it is not possible to determine the activation overpotential which leads to the breaking of either the CO–Ru or OH–Ru bonding for the initiation of CO_{ad} oxidation. However, the adsorbed CO species are still present at the pre-oxidation region (below + 0.85 V) and possess high mobility based on the low adsorption energy of CO on an O–(1 × 1)–Ru (0001) surface [110]. The oxidation processes for CO oxidation can be described according to the following equations:

$$OH^-_{bulk} + * \rightarrow OH^-_{ad} \quad (3.1)$$

$$OH^-_{ad} \rightarrow OH_{ad} + e^- \quad (3.2)$$

$$OH_{ad} + CO_{ad} \rightarrow CO_2 + H^+ + e^- + 2*, \quad (3.3)$$

where * indicates a vacant site on Ru (0001) and the subscript $_{ad}$ the adsorption on Ru (0001).

In the first step, the bulk OH^- ion is electrosorbed onto the Ru electrode surface by migration/diffusion. The overpotential of step 3.2, known as the activation overpotential, is most likely rate determining, leading to discharge and breaking of the O/OH–Ru bond, as demonstrated by the pronounced transient current of CO oxidation at + 0.85 V on a Ru (0001) [109]. Since the binding energy (+ 5.07 eV) of O–Ru on a (1 × 1)–O hexagonal close-packed (hcp) [111] is approximately 10 times larger than the binding energy (+ 0.48 eV) of CO–Ru on a (1 × 1)–O surface [110], the overall reaction spontaneously occurs when the OH–Ru bond is broken *via* step 3.3.

On the other hand, the different onset potential of CO oxidation observed at different cycles of CO stripping voltammetry can be ascribed to the change in CO coverage on the Ru (0001) surface, as demonstrated by the following. In Figure 3.7(a), a lower onset potential (+ 0.55 V) of CO oxidation on the second cycle obviously results from the reaction of the weakly adsorbed O species with CO_{ad}, in which the CO

coverage has been decreased by the first CO stripping cycle. It is clearly confirmed by an additional CO stripping measurement (see Figure 3.7(b)) on Ru (0001) with a lower coverage of CO adsorbate (*ca.* 0.2 ML). Since the coverage of CO in Figure 3.7(b) is close to the remaining CO coverage on a Ru (0001) surface after the first CO stripping cycle (see Figure 3.7(a)), the first onset of CO oxidation is also observed at + 0.55 V (as shown in Figure 3.7(b)). This clearly demonstrates that the onset of CO oxidation depends on the CO coverage on a Ru (0001). The oxidative removal of CO_{ad} during the first cycle can apparently result in the adsorption of O and it is proven by the reduction peak of oxygen at + 0.17 V on the negative-going scan. The partial removal of CO_{ad} and O_{ad} species in the first cycle increases the coverage of surface oxygen and the O/CO ratio in the second cycle (see Figure 3.7(a)), whereby the adsorption energy of CO_{ad} is significantly decreased [110, 113] and the bonding energy of O–Ru becomes smaller from 5.87 eV on O–(2 × 2) to 5.07 eV on O–(1 × 1) [112]. Thus, the onset of CO oxidation occurs at a lower overpotential in the next anodic scan. Partial removal of CO accompanied by O adsorption has also been confirmed by *in-situ* IR measurements which show an increase of ν_{CO} with the increasing potential [114] that is characteristic of CO adsorbed in the presence of surface oxygen on Ru (0001) under UHV conditions [112], *e.g.*, the stretching band of C–O increased from 2010 cm^{-1} at 0.0 V to 2040 cm^{-1} at + 0.8 V [114].

Electro-oxidation of CO on a rough Ru (0001) surface

A rough Ru (0001) surface with numerous defects, kinks and facets has a significantly higher electrocatalytic activity for CO oxidation than a flat Ru (0001) surface. The CO oxidation commences at a lower overpotential of + 0.15 V and a pronounced broad peak appears at + 0.35 V, where there is no measurable CO oxidation peak on a flat Ru (0001) surface. This is similar to the results at a Pt electrode. The pronounced CO stripping peak on the rough Ru (0001) surface is broader than the CO oxidation peak on a Pt (111) surface [115, 116] and it indicates that this broad peak consists of the superposition of different CO stripping peaks on various facets of the rough Ru (0001) surface. Moreover, the CO adspecies was almost completely oxidised in the first anodic cycle, which is similar to CO oxidation on a Pt (111) [112] and a Ru-modified Pt (111) surface [106]. The reason for the high catalytic activity of a rough

Ru (0001) surface may be attributed to the formation of oxide layers on various facet planes and it is also due to the higher mobility of Ru atoms on the rough Ru surface. The latter has been demonstrated by the RHEED pattern obtained for the Ru electrode after CO electro-oxidation, showing the sharpening of the reflection rods of the Ru substrate; *i.e.*, the smoothing of the rough Ru surface induced by CO oxidation. On the other hand, ion sputtering at room temperature generates various facet planes (hkl), leading to the formation of different oxide layers on (hkl) planes, some of which apparently have a higher catalytic activity towards CO oxidation. The mobility of Ru atoms was enhanced by the oxidation/adsorption of CO, facilitating the breaking of the Ru-O bond and the reaction with co-adsorbed CO *via* a Langmuir-Hinshelwood mechanism. Both the higher mobility of Ru atoms and the formation of the oxide layers on various facets can induce the higher electrocatalytic activity for CO oxidation.

The process of CO electro-oxidation differs remarkably from the gas phase CO oxidation on Ru (0001) surfaces at high pressure or under UHV conditions where the bonding energy of O–Ru is too strong to allow reaction with the weakly adsorbed CO on the Ru (0001) surface at room temperature [112, 113, 116]. Weakening of the O–Ru bond by infrared femtosecond laser pulses leads to CO_2 formation on a O + CO covered Ru (0001) surface [117]. This is similar to the electro-oxidation of CO on a flat Ru surface by increasing the oxidation overpotential, when the O–Ru bond becomes weaker. On the other hand, the electro-oxidation of CO on a rough Ru (0001) surface occurs at lower oxidation overpotentials and is due to the weak bonding energy of O–Ru caused by enhanced oxide layers on (hkl) facets.

3.3.6 Electro-oxidation of formic acid on a Ru (0001) surface

After examining CO oxidation, we now turn to oxidation of formic acid (HCOOH) on Ru, during which CO is formed as an intermediate. In contrast to methanol on Ru, there is a strong interaction of Ru with formic acid. It was suggested in a previous study [118] that the interaction was primarily dehydration leading to adsorbed CO (see first part of Eq. (3.4)).

$$HCOOH \rightarrow CO_{ad} + H_2O \quad (3.4)$$

$$\rightarrow CO_2 + 2H^+ + 2e^- .$$

Figure 3.10 shows the cyclic current-potential curve of flat Ru (0001) in 0.1 M HCOOH/0.1 M $HClO_4$ solution with a scan rate of 50 mV/s. Two reduction peaks on the cathodic scan and one oxidation peak of CO on the anodic scan were clearly observed (the nature of the 2nd cathodic peak at 0.0 V is not clear, it may represent a replacement of adsorbed OH by CO or involve reduction of formic acid). Comparing with data measured at a temperature of 50 °C by Lin *et al*. [119], the distinct anodic peak indicating HCOOH oxidation at an overpotential of + 0.6 V is clearly observed, even though experiments were performed at room temperature. According to the dual-path mechanism for formic acid oxidation [118] represented by Eq. (3.4), dehydration of formic acid could occur at a low overpotential.

This CV profile is in accordance with current-potential profile in CO-saturated $HClO_4$ solution (not shown), since the oxidation of HCOOH could be similar to CO oxidation according to Eq. (3.4). It can be concluded that the major pathway for HCOOH oxidation on Ru is not *via* the dehydration of the molecule (Eq. 3.4) but *via* its dehydrogenation (Eq. 3.5).

$$HCOOH \rightarrow CO_2 + 2H^+ + 2e^- . \quad (3.5)$$

It is well understood that the reaction on Pt at a low potential appears to proceed primarily by the direct step (dehydrogenation, see Eq. (3.4)) to yield CO_2 and water, and CO accumulates on the Pt surface as a side reaction, *i.e.*, is truly a poison. While the dehydrogenation of HCOOH is predominant on pure Pt, the major reaction pathway on pure Ru is dehydration leading to adsorbed CO, which then can be oxidised at potentials which agree with the measured peak potentials in CO stripping voltammetry in a CO-saturated solution. This different observation between Pt and Ru in their electrochemical interactions with formic acid, namely the affinity of Pt towards the dehydrogenation reaction (with an estimated CO_2/CO branching ratio of *ca.* 10^2) and the affinity of Ru for dehydrations is reflected in comparable affinities in the interactions of formic acid with these surfaces in vacuum [120, 121]. In the previously proposed mechanism of

action [84], Ru provides sites that oxidise CO at much lower potentials than Pt, which should, in principle, result in a much lower steady state level of CO on the surface.

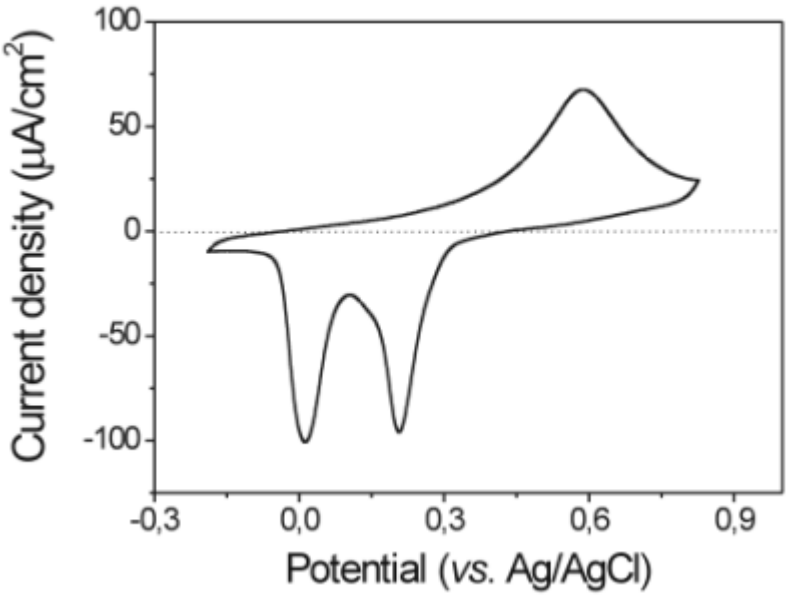

Figure 3.10. Cyclic voltammetry for HCOOH oxidation on a flat Ru (0001) electrode in 0.1 M HCOOH/0.1 M $HClO_4$. Scan rate is 50 mV/s.

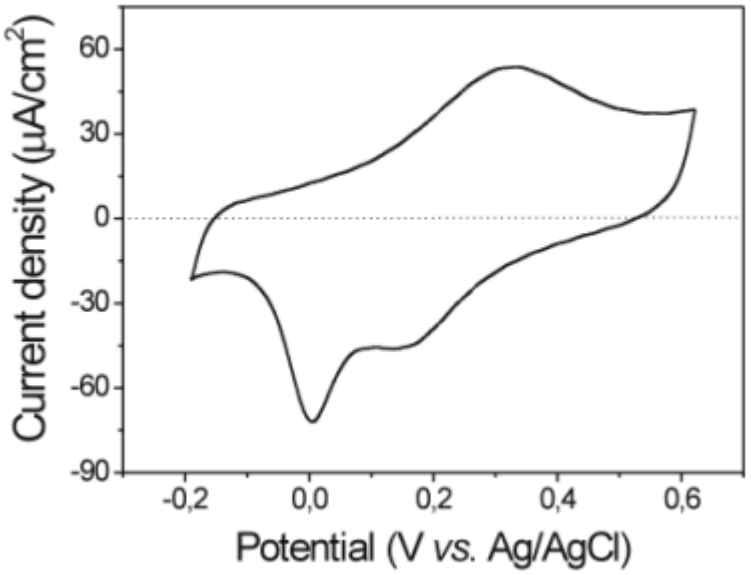

Figure 3.11. Cyclic voltammetry for HCOOH oxidation on a rough Ru (0001) electrode in 0.1 M HCOOH/0.1 M $HClO_4$. Scan rate is 50 mV/s.

Summarising the above mechanistic understanding of formic acid oxidation and analysing CO oxidation behaviour on both flat and rough Ru (0001) surfaces in the previous section, one can apply similar arguments for HCOOH oxidation; HCOOH oxidation on a rough Ru surface occurs at a much lower overpotential compared with that on the flat Ru surface. Figure 3.11 is a CV on a rough Ru (0001) electrode. The highest oxidation rate of HCOOH on a rough Ru (0001) surface occurs at a much lower overpotential of + 0.32 V compared with the pronounced anodic peak (+ 0.6 V) on the flat surface. Interestingly, the oxidation of HCOOH on a rough Ru surface commences at *ca.* 0.0 V, indicated by the onset of oxidation currents in the cyclic voltammetry. This also supports the above hypothesis that a rough Ru surface has a higher electrocatalytic activity for the oxidation of HCOOH.

3.4 Summary

In the cyclic voltammetry (CV) curve on a flat Ru (0001) surface in 0.1 M $HClO_4$ solution, distinct adsorption/desorption peak pairs of hydrogen (H) and O/OH have been observed. However, the CV on a rough Ru (0001) surface showed a featureless profile induced by the overlapping of current peaks on various facet planes. Three different onset potentials of CO oxidation at +0.86 V, + 0.55 V and + 0.46 V observed on the subsequent three CVs are probably related with differences in OH adsorption and different binding states in the O/CO coadsorbates. The onset of CO oxidation on a flat Ru (0001) surface was at + 0.5 V on the first anodic scan, while the oxidation of adsorbed CO on a rough Ru (0001) set in at a lower overpotential of + 0.15 V and a pronounced broad oxidation peak was observed at + 0.35 V. The rate of CO oxidation was most likely determined by the strength of the O-Ru bond, whereby the O species reacted with the adsorbed CO *via* a Langmuir-Hinshelwood mechanism. The adsorbed CO on rough Ru (0001) was completely oxidised during the first anodic scan.

In the electrocatalytic oxidation of HCOOH, the CV on flat Ru (0001) resembles the CV for CO oxidation in a CO-saturated solution. It means that on a Ru (0001) surface, formic acid most likely oxidised through the indirect oxidation path, *i.e.*, CO is an intermediate species in HCOOH oxidation. Formic acid oxidation on rough

Ru (0001) set in at a lower overpotential compared with a flat Ru (0001) surface. These results showed that a rough Ru surface has a higher electrocatalytic activity compared with a flat Ru (0001) surface.

Chapters 4 to 6 describe the oxidation behaviours of more complex organic molecules, namely formic acid and methanol, on Pt surfaces with and without the modification of foreign adatom. In all cases, CO plays an important role as an intermediate.